

Structure and dynamics in glass-formers: predictability at large length scales

Ludovic Berthier

*Joint Theory Institute, Argonne National Laboratory and University of Chicago, 5640 S. Ellis Av., Chicago, IL 60637**

Robert L. Jack

Department of Chemistry, University of California, Berkeley, CA 94720-1460

(Dated: February 5, 2008)

Dynamic heterogeneity in glass-formers has been related to their static structure using the concept of dynamic propensity. We re-examine this relationship by analyzing dynamical fluctuations in two atomistic glass-formers and two theoretical models. We introduce quantitative statistical indicators which show that the dynamics of individual particles cannot be predicted on the basis of the propensity, nor by any structural indicator. However, the spatial structure of the propensity field does have predictive power for the spatial correlations associated with dynamic heterogeneity. Our results suggest that the quest for a connection between static and dynamic properties of glass-formers at the particle level is vain, but they demonstrate that such connection does exist on larger length scales.

PACS numbers: 05.10.-a, 05.20.Jj, 64.70.Pf

The future ain't what it used to be—Y. Berra

I. INTRODUCTION

Supercooled liquids near the glass transition have paradoxical physical properties [1, 2]. They exhibit a range of peculiar dynamical features that have been attributed to spatially heterogeneous dynamical relaxation [2, 3, 4, 5, 6, 7, 8, 9, 10, 11], but their structure, as measured by two-point correlation functions, appears homogeneous and unspectacular. Theoretical pictures of the glass transition assume different kinds of connections between static and dynamic properties. For example, in a picture based on dynamical facilitation [5, 12], one postulates the existence of mobile and immobile regions, with the implicit assumption that these regions have a structural origin. Frustration-based theories [13] infer dynamical behavior by assuming the existence of domains with a preferred local order. Alternatively, one can attempt to connect static and dynamical properties through the configurational entropy [14, 15], through two-point density correlations [16], through elastic properties [17, 18], or through the idea of a rough energy landscape [7, 19]. The extent to which these connections can be objectively established in experiments and computer simulations is an important criterion for evaluating different theoretical pictures.

To address this point, Harrowell and co-workers introduced the isoconfigurational ensemble [20], which isolates the effect of the liquid structure on its dynamical fluctuations. In this statistical ensemble, dynamical observ-

ables known as ‘propensities’ are obtained by averaging over independent trajectories from the same initial configuration. Fixing the initial particle positions preserves structural information on all length scales, and allows the influence of structure to be separated from intrinsically dynamical fluctuations. The difficult task of connecting structure to dynamics is then broken into two seemingly simpler ones: first connect structure to propensity, then propensity to dynamics.

This idea has been exploited in several works [20, 21, 22, 23, 24, 25, 26, 27], which focussed primarily on the first stage of the problem, and aimed at finding correlations between propensity and local or non-local structural quantities. In this paper, we concentrate instead on the second stage, the connection between propensity and dynamics, which has received relatively little attention. After all, if propensity and dynamics only had weak connections, the isoconfigurational ensemble would not be such a useful tool. The isoconfigurational average preserves all fluctuations that have any connection to the initial structure, but fluctuations whose origin is inherently dynamical are averaged away. Thus, propensities capture the physically relevant dynamical fluctuations if and only if these fluctuations are structural in origin [20], in which case dynamics can be predicted from knowledge of the structure. In concentrating on the connection between structure and propensity, previous works [22, 23, 24, 25, 26, 27] have assumed that this is indeed the case.

Here, we analyze quantitatively the implicit assumption of predictability. We establish that the dominant single-particle dynamical fluctuations are intrinsically dynamical, and not linked with liquid structure. However, we find that the sizes and shapes of mobile and immobile regions can be predicted from the propensity, and these collective dynamical fluctuations do indeed have a structural origin. Although the relevance of intrinsically dynamical fluctuations has been discussed in a qualita-

*Permanent address: Laboratoire des Colloïdes, Verres et Nanomatériaux, UMR 5587, Université Montpellier II and CNRS, 34095 Montpellier, France

tive way by Widmer-Cooper and Harrowell [20, 21], the subtle length scale dependence of the correlation between structure and dynamics, and therefore of predictability, was not discussed nor anticipated in previous work.

After defining our models in Sec. II, we discuss single particle and collective dynamics in Secs. III and IV, combining illustrative snapshots with quantitative analysis, and comparing our results with the behavior in schematic models. We conclude in Sec. V, and identify directions for future study.

II. MODELS

We present numerical data for two atomistic glass-formers: a Lennard-Jones (LJ) binary mixture [28], and a model of silica due to Beest, Kramer and van Santen (BKS) [29]. We use Monte Carlo dynamics, which have been shown to yield a dynamical behavior in excellent agreement with Newtonian dynamics when time is scaled appropriately [30, 31]. We measure time in Monte Carlo sweeps, and other units are as in Refs. [30, 31]. The LJ system has 1000 particles, and we study temperatures between 1.0, where the system is a simple liquid, and 0.47, where the relaxation time has increased by a factor of approximately 1000, and the system is in the glassy regime. For reference the mode-coupling temperature for this system is $T_c = 0.435$. The BKS system has 1008 atoms, and the relaxation time also spans around three decades, from a liquid state around 6000 K to a glassy one around 3000 K.

We also study the one-spin facilitated Fredrickson-Andersen (1-FA) model [12], using Monte Carlo simulations. It represents a simple model of a dynamically heterogeneous material, with a few mobile regions that facilitate motion in immobile regions nearby [5]. Defining spins $n_i \in \{0, 1\}$ on the site of a lattice, we identify sites with $n_i = 1$ as ‘mobile’ and those with $n_i = 0$ as ‘immobile’. The dynamics of the system obey detailed balance with respect to a trivial energy function $E = \sum_i n_i$. The non-trivial behavior of the model comes from a dynamical constraint: spins are allowed to flip only if at least one of their neighboring sites is mobile. At low temperatures, $T < 1$, and low spatial dimension, $d < 2$, the model displays glassy features such as transport decoupling [32] and an increasing dynamical length scale [6].

We use $C_i(t)$ to denote a general dynamical object attached to particle i , such as $f_i(t) \equiv \cos(\mathbf{k} \cdot [\mathbf{r}_i(t) - \mathbf{r}_i(0)])$ or $\mu_i(t) \equiv |\mathbf{r}_i(t) - \mathbf{r}_i(0)|$. For $f_i(t)$, we use $|\mathbf{k}| = 6.7$ for the LJ model and $|\mathbf{k}| = 1.8 \text{ \AA}^{-1}$ for silica. These wave vectors correspond to the location of the first diffraction peak in the LJ system, and to the pre-peak of the structure factor of silica. The quantity $f_i(t)$ is therefore a measure of local relaxation in these liquids. In lattice models, we consider $P_i(t)$, the persistence function on site i , which takes the value of unity if spin i has not flipped in the interval $[0, t]$, and zero otherwise.

We define an isoconfigurational average $\langle \dots \rangle_{\text{iso}}$ in

which the initial positions of all particles are held fixed [20], but dynamical trajectories are made independent through the use of different random numbers in the Monte Carlo trajectories [25]. The dynamic propensity is then defined by $\langle C_i(t) \rangle_{\text{iso}}$ [20]. Equilibrium ensemble averages are denoted by $\mathbb{E}[\dots]$. As usual, we define the structural relaxation time τ_α by $\mathbb{E}[f_i(\tau_\alpha)] = 1/e$.

III. SINGLE PARTICLE DYNAMICS

A. Atomistic systems

We begin with a qualitative analysis of fluctuations within the isoconfigurational ensemble. Fig. 1 shows a scatter plot for the LJ system, comparing squared particle displacements in a single run, $\mu_i^2(t)$, with their corresponding propensities, $\langle \mu_i^2(t) \rangle_{\text{iso}}$. Points near the dashed line represent particles whose displacements in this single run are close to their isoconfigurational averages. Given the large scatter seen in Fig. 1, it is clear that the propensity cannot be used to predict the actual value of the displacement in a single run. That is, even when all aspects of the initial structure are held constant, there are large fluctuations in the single-particle dynamics, which appear to be more important than particle-to-particle fluctuations of the propensity. These large dynamical fluctuations mean that the propensities have very little predictive power for the single-particle dynamics.

Fig. 1 also shows the distribution of particle (logarithmic) displacements, $P(\log \mu)$, and of propensities, $P(\log \langle \mu \rangle_{\text{iso}})$. The former, which is directly related to the

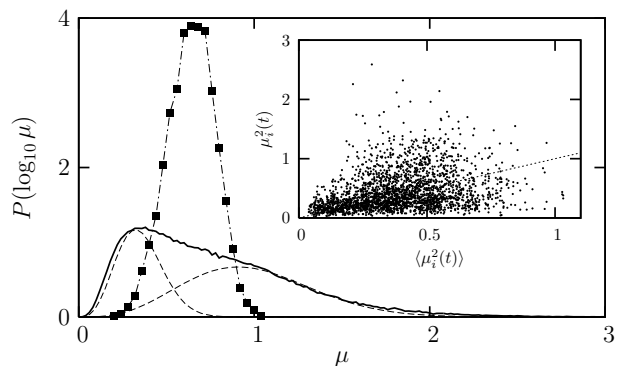


FIG. 1: Data for the LJ system in the glassy regime ($T = 0.47$). Inset: Scatter plot, comparing squared displacements in a single run, $\mu_i^2(\tau_\alpha)$, with their average over runs from the same initial condition, $\langle \mu_i^2(\tau_\alpha) \rangle_{\text{iso}}$. Note that the lack of correlation between propensity and dynamics necessitates the use of different scales on the two axes. The dotted line is $\mu_i^2(\tau_\alpha) = \langle \mu_i^2(\tau_\alpha) \rangle_{\text{iso}}$. Main: The broad distribution of particle (logarithmic) displacements, $P(\log \mu)$ (full line) arises from the coexistence of mobile and immobile particles, illustrated with dashed lines (Gaussian distributions). This is compared with the much narrower distribution of propensities, $P(\log \langle \mu \rangle_{\text{iso}})$.

van-Hove function, has a broad, non-Gaussian shape, reflecting the coexistence of mobile and immobile particles in the liquid [3, 11], as illustrated by fitting the large- μ and small- μ parts of the distribution with two distinct Gaussian distributions. The latter distribution (particle propensities) is much narrower and structureless. In particular, the distinction between fast and slow particles is no longer apparent. This most distinctive feature of dynamic heterogeneity [2] is therefore not structural in nature, but is intrinsically dynamical.

The details of the distribution of the propensity shown in Fig. 1 are different from those shown in [20, 21]. We attribute this to differences between our model systems (in particular their different dimensionalities and tendencies to crystallize), and to our use of slightly different observables (we use simple distances while squared distances were used in [20, 21], emphasizing particles with large displacement). For our purposes, the important feature is that the distribution of propensities is much narrower than that of bare displacements, which is consistent with earlier results [33].

We now support these qualitative statements by quantitative measures. In order to disentangle structural and dynamical sources of fluctuations, we define three variances:

$$\begin{aligned}\delta_C(t) &= \mathbb{E}[\langle C_i(t) \rangle_{\text{iso}}^2] - \mathbb{E}^2[C_i(t)], \\ \Delta_C^{\text{iso}}(t) &= \mathbb{E}[\langle C_i^2(t) \rangle_{\text{iso}} - \langle C_i(t) \rangle_{\text{iso}}^2], \\ \Delta_C(t) &= \mathbb{E}[\langle C_i^2(t) \rangle_{\text{iso}}] - \mathbb{E}^2[C_i(t)],\end{aligned}\quad (1)$$

so that $\Delta_C(t) = \Delta_C^{\text{iso}}(t) + \delta_C(t)$; we use the short-hand notation $\mathbb{E}^2[\dots] = (\mathbb{E}[\dots])^2$ and the subscript indicates the dynamic observable of interest. Thus, $\delta_C(t)$ measures particle to particle fluctuations of the propensity [23] and captures the structural component of the fluctuations. $\Delta_C^{\text{iso}}(t)$ measures the fluctuations of $C_i(t)$ between different runs at fixed initial configuration and captures therefore the dynamical component of the fluctuations. Their sum $\Delta_C(t)$ naturally measures the total amount of fluctuations.

These quantities are defined in the same spirit as the ensemble-dependent susceptibilities of Refs. [10]. To assess the influence of a given variable (the structure) on the fluctuations measured by $\Delta_C(t)$, we use a constrained statistical ensemble (the isoconfigurational ensemble) where this variable is kept fixed, and measure a ‘restricted’ variance, $\Delta_C^{\text{iso}}(t)$. The difference between restricted and unrestricted variances is $\delta_C(t)$, which accounts for the fluctuations of the restricted variable [10]. In our case, the relative sizes of $\delta_C(t)$ and $\Delta_C^{\text{iso}}(t)$ quantify the relative influence of structural and dynamical fluctuations. It is natural to introduce the dimensionless ratio

$$R_C(t) = \frac{\delta_C(t)}{\Delta_C(t)}, \quad (2)$$

with $0 \leq R_C(t) \leq 1$. Small values of $R_C(t)$ mean that the structure has little effect on the single particle dynamics,

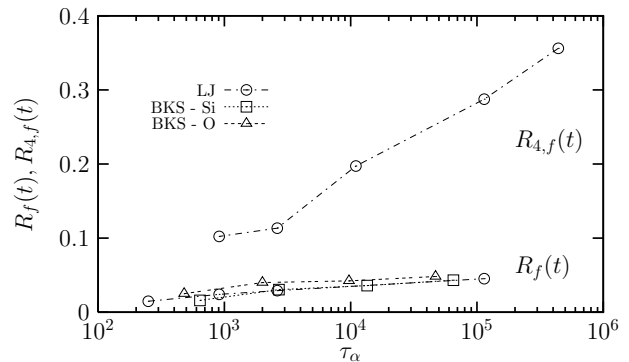


FIG. 2: Ratios $R_f(\tau_\alpha)$ for the LJ and silica systems, and $R_{4,f}(\tau_\alpha)$ for the LJ system. Temperatures are $0.47 \leq T \leq 1.0$ (LJ) and $3000\text{K} \leq T \leq 6100\text{K}$ (BKS). $R_f(t)$ is small and grows slowly with decreasing T , while $R_{4,f}(t)$ is large and grows steadily. This suggests that connections between structure and dynamics are only significant on large length scales.

large values mean instead that structure is a very good predictor of the dynamics.

We present results for the ratio $R_f(\tau_\alpha)$ for LJ and BKS glass-formers in Fig. 2. This ratio vanishes at high T , and grows slowly as τ_α increases, reaching about 4% in both systems at the lowest temperature studied (when τ_α has grown by about 3 decades). The smallness of $R_f(\tau_\alpha)$ confirms the impression gained from Fig. 1: structure at time 0 has little influence on the dynamics of individual particles at times τ_α .

B. Comparison with a schematic model

It is instructive to evaluate $R_C(t)$ in a simple model of a dynamically heterogeneous liquid. We suppose that particles diffuse independently with diffusion constants D_i that depend on their initial environments. We also assume that effects of the initial environment decay on timescales comparable with τ_α . Then, each particle has $\langle f_i(t) \rangle_{\text{iso}} = e^{-D_i k^2 t}$, and

$$F(t) \equiv \mathbb{E}[f_i(t)] = \int_0^\infty d\lambda g(\lambda) \exp(-\lambda t), \quad (3)$$

where $\lambda_i = D_i k^2$ is a rescaled diffusion constant distributed according to $g(\lambda)$. Using the definition of $f_i(t)$, we have $f_i(t)^2 = (1/2)\{\cos(2\mathbf{k} \cdot [\mathbf{r}_i(t) - \mathbf{r}_i(0)]) - 1\}$, and we find

$$\begin{aligned}\delta_f(t) &= F(2t) - F^2(t), \\ \Delta_f(t) &= (1/2)[1 + F(4t) - 2F^2(t)].\end{aligned}\quad (4)$$

In a dynamically homogeneous system, all particles have the same diffusion constant, $F(t)$ decays exponentially, and $\delta_f(t) = 0 = R_f(t)$. On the other hand, consider a heterogeneous system with equal populations

of fast and slow particles, whose rescaled diffusion constants are λ_1 and λ_2 . Using Eq. (3), this leads to a two-step decay: $F(t) = (1/2)[e^{-\lambda_1 t} + e^{-\lambda_2 t}]$. In this case, $R_f(t)$ has a non-monotonic time dependence, vanishing at small and long times, with a maximal value near 50% during the plateau of $F(t)$ (that is, for times such that $\lambda_1^{-1} \ll t \ll \lambda_2^{-1}$). This indicates that correlations between structure and dynamics are generically maximal during plateaux of $F(t)$ [23]; our atomistic simulations are also consistent with this indication.

Our analysis of this highly schematic model demonstrates that large values of $R_f(t)$ are obtained in the presence of reproducibly fast and slow particles. Comparing this reference theory with the small values for $R_f(t)$ shown in Fig. 2, it follows that the correlation between structure and single-particle dynamics is weak in atomistic systems and does not seem to dramatically increase when temperature gets smaller.

We conclude that the search for a connection between static and dynamic properties at the single-particle level is in vain. Certainly, no such connection has been found [20, 21, 22, 23, 24, 25, 26, 27].

IV. COLLECTIVE DYNAMICS

Having ruled out the structural origin of one important aspect of dynamic heterogeneity, we now address a different question: Do spatial fluctuations of the propensity carry meaningful information on the geometry and spatial extent of the dynamic heterogeneities in supercooled liquids? We will show that while it is not possible to use the structure to predict whether a given particle will be fast or slow in a single run, it is possible to tell if it belongs to a fast or slow *region*.

A. LJ system

We begin by generalizing the variances in (1) to those of global dynamic quantities, $C_g(t) = N^{-1} \sum_i C_i(t)$. We define:

$$\begin{aligned} \delta_{4,C}(t) &= N \{ \mathbb{E} [\langle C_g(t) \rangle_{\text{iso}}^2] - \mathbb{E}^2 [C_g(t)] \}, \\ \chi_{4,C}^{\text{iso}}(t) &= N \{ \mathbb{E} [\langle C_g^2(t) \rangle_{\text{iso}}] - \langle C_g(t) \rangle_{\text{iso}}^2 \}, \\ \chi_{4,C}(t) &= N \{ \mathbb{E} [\langle C_g^2(t) \rangle_{\text{iso}}] - \mathbb{E}^2 [C_g(t)] \}, \end{aligned} \quad (5)$$

with $\chi_{4,C}(t) = \delta_{4,C}(t) + \chi_{4,C}^{\text{iso}}(t)$. The usual four-point susceptibility $\chi_{4,C}(t)$ measures the size of collective dynamical fluctuations [8, 9]. By analogy with $\delta_C(t)$ and $\Delta_C^{\text{iso}}(t)$, we identify $\delta_{4,C}(t)$ as the contribution to $\chi_{4,C}(t)$ associated with the structure, and $\chi_{4,C}^{\text{iso}}(t)$ as the intrinsically dynamical contribution. Then, in analogy with $R_C(t)$,

$$R_{4,C}(t) = \frac{\delta_{4,C}(t)}{\chi_{4,C}(t)}, \quad (6)$$

is a dimensionless measure of the effect of the structure on collective aspects of the dynamics. In Fig. 2, we show that the contribution of $\delta_{4,f}(\tau_\alpha)$ to the dynamic fluctuations is about 35% at $T = 0.47$ (to be compared to the 4% found for single particle heterogeneity). Moreover, $R_{4,f}(\tau_\alpha)$ grows steadily when T decreases. This quantitative measurement shows that when the system is in the glassy regime, collective dynamical fluctuations are indeed quite reproducible in repeated runs from the same initial configuration. We conclude that connections between structural and dynamical properties are significant on these length scales, and that the connection even gets stronger as the relaxation time increases.

To investigate the fluctuations associated with this effect, we interpolate between the single-particle and collective dynamics, by averaging over a length scale ℓ :

$$\overline{C}_i(t, \ell) = \frac{\sum_j C_j(t) h(|\mathbf{r}_i - \mathbf{r}_j|)}{\sum_j h(|\mathbf{r}_i - \mathbf{r}_j|)}, \quad h(x) = e^{-(x/\ell)^2}. \quad (7)$$

By coarse-graining in this way, we can investigate how the reproducibility of dynamical fluctuations varies with length scale.

In Fig. 3, we use snapshots of the system to illustrate that large scale features of the dynamics are indeed reproducible from run to run. For a representative initial configuration at a low temperature, Fig. 3a shows the LJ particles with the largest values of the propensity $\langle f_i(\tau_\alpha) \rangle_{\text{iso}}$ (these are the particles which are slow on average). In all panels of Fig. 3, we show about 1/3 of the particles: this threshold is small enough to give clear images, but large enough to avoid placing undue emphasis on rare fluctuations.

Figs. 3b-d show particles with the largest values of $\overline{f}_i(t, \ell = 1)$ in three individual runs. Loosely speaking, the coarse-graining scale $\ell = 1$ means that \overline{f}_i measures how much motion is associated with a particle and its nearest neighbors, on the time scale t (the choice of this length scale is discussed below). Thus, Figs. 3b-d show particles that are located in a relatively immobile environment during these three trajectories. Similar clusters of immobile particles are apparent in all three trajectories, and these clusters correlate quite well with the cluster of slow particles that is observed in the propensity map in Fig. 3a. Since the slow behavior of these clusters is reproducible in independent runs from the same initial condition, it surely must have a structural origin. This is consistent with the rather strong coupling of structure and collective dynamics that was identified in Fig. 2. We also note in passing that the coarse-grained pictures in Figs. 3b-d are computationally much cheaper than calculating the propensity field.

As discussed above, the coupling between structure and dynamics at the single-particle level is weak. This is further illustrated in Fig. 3e, where we have not coarse-grained, but simply identified slow particles by their values of $f_i(\tau_\alpha)$, again using the same initial condition. In this case the immobile cluster that is apparent in Fig. 3a-d is obscured by large intrinsically dynamical fluctua-

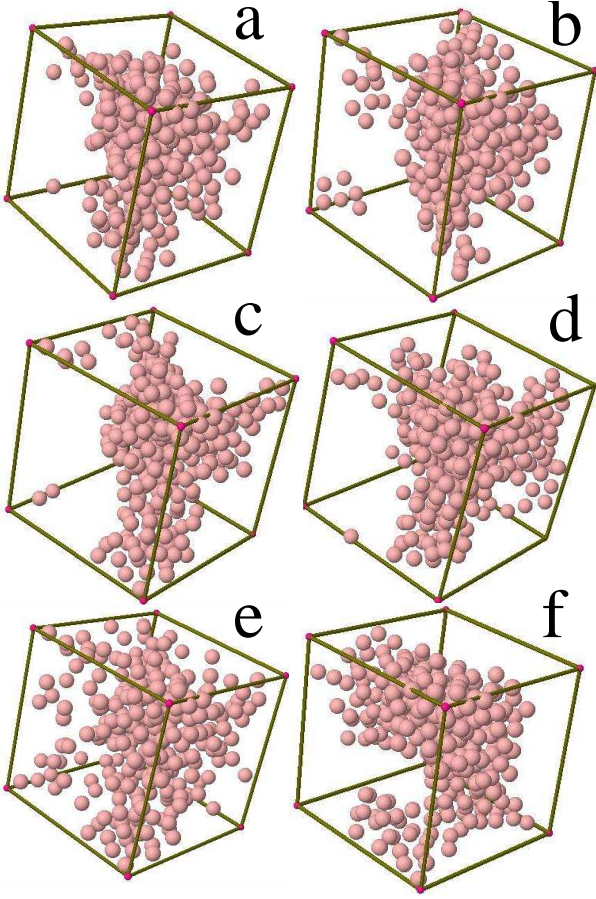


FIG. 3: a: Image of the 300 particles with the smallest propensity for motion (largest values of $\langle f_i(\tau_\alpha) \rangle_{\text{iso}}$), for a representative initial condition in the LJ system in the glassy regime ($T = 0.47$). b-d: Images of the 300 particles with largest values of the coarse-grained observable $\bar{f}_i(\tau_\alpha, \ell = 1)$, in three representative runs from the same initial condition. Spatial structure similar to that of (a) is found in all cases. e: As (c), without coarse-graining ($\ell = 0$). f: Image of the 300 particles with the smallest values of the coarse-grained potential energy, $\bar{e}_i(\ell = 2)$, for the same configuration. The resulting structure is correlated with that of (a).

tions. Comparing Fig. 3e with Figs. 3b-d shows that the effect of coarse-graining on the short length scale $\ell = 1$ is quite effective in suppressing these fluctuations, allowing the slow cluster to become apparent. When coarse-graining in this way, we must also ensure that the length scale ℓ is smaller than the correlation length associated with the dynamically correlated clusters, or else these clusters will themselves be obscured. We establish below (Fig. 4) that the dynamically correlated clusters have a length scale $\xi^{\text{prop}} \simeq 2$ at this temperature. Thus, while it would be desirable to have well-separated length scales ℓ and ξ^{prop} , we can at least establish that $\ell < \xi^{\text{prop}}$, as required for the consistency of our analysis. As expected, we find that on further increasing the coarse-graining scale ℓ , the structure of the immobile clusters in Figs. 3b-d is still apparent, but the ability to resolve

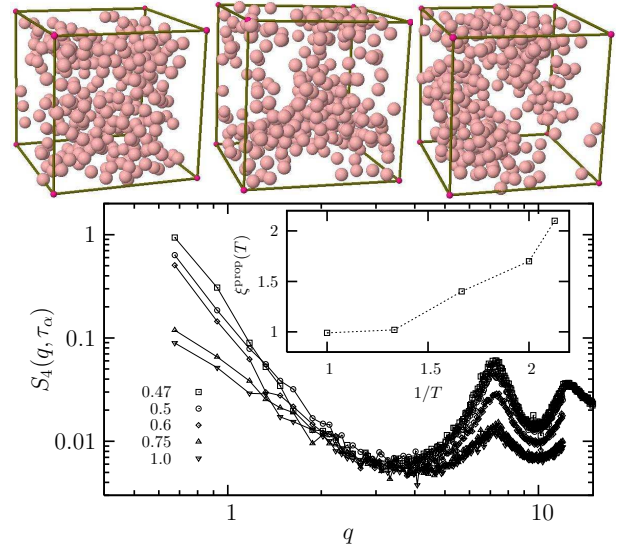


FIG. 4: Top: Images of the 300 particles with the largest values of $\langle f_i(\tau_\alpha) \rangle_{\text{iso}}$ at $T = 1.0, 0.6$, and 0.47 (left to right) in the LJ system. Increasing clustering of propensity fluctuations is evident. Bottom: Structure factor of propensity fluctuations at several T . The inset shows the extracted lengthscale $\xi^{\text{prop}}(T)$, which grows as the temperature decreases.

their shape is lost.

Returning to the spatial correlations of the propensity, we interpret $\delta_{4,f}(t)$ as a dynamic susceptibility associated with spatial fluctuations of the propensity, by analogy with the four-point susceptibility $\chi_{4,f}(t)$ [8, 9]. That is, defining the fluctuations of the propensity by $\langle \delta f_i(t) \rangle_{\text{iso}} = \langle f_i(t) \rangle_{\text{iso}} - F(t)$, then the spatial correlation function of the propensity is

$$G_4^{\text{prop}}(\mathbf{r}, t) = \mathbb{E} \left[N^{-1} \sum_{ij} \langle \delta f_i(t) \rangle_{\text{iso}} \langle \delta f_j(t) \rangle_{\text{iso}} \times \delta(\mathbf{r}_i(0) - \mathbf{r}_j(0) - \mathbf{r}) \right]. \quad (8)$$

The associated structure factor is the Fourier transform of this function:

$$S_4^{\text{prop}}(\mathbf{q}, t) = \int d\mathbf{r} e^{i\mathbf{q} \cdot \mathbf{r}} G_4^{\text{prop}}(\mathbf{r}, t), \quad (9)$$

and the associated dynamical susceptibility is $\delta_{4,C}(t) = S_4^{\text{prop}}(q \rightarrow 0, t)$. By analogy with the four-point susceptibility, we expect $\delta_{4,C}(t)$ to be proportional to the number of particles associated with collective fluctuations of the propensity.

Like $\chi_4(t)$, the susceptibility of the propensity $\delta_{4,C}(t)$ is a non-monotonic function of time that peaks near τ_α . We find that the height of this peak grows as T decreases, suggesting increasing spatial correlations of the propensity. This is illustrated by the images in Fig. 4, which show that the particles with smallest propensities are increasingly spatially clustered as T decreases. To confirm this visual impression, we present in Fig. 4 our numerical

data for $S_4^{\text{prop}}(q, t)$ measured at different temperatures in the LJ system. The structure factor of the propensity is similar to the structure factor of dynamic heterogeneity, with the striking appearance of a small- q peak. Following earlier work we estimated [34] the correlation length of propensity fluctuations $\xi^{\text{prop}}(T)$, as shown in the inset of Fig. 4. It has a clear, but rather slow, growth when T decreases, compatible with determinations of a typical lengthscale of dynamic heterogeneity [5, 9, 10].

These measurements confirm that spatial correlations of the propensity increase when temperature decreases, just as the length scale of dynamic heterogeneity does. Therefore, we find the intriguing result that the value of the propensity of any individual particle is only weakly correlated to its dynamical behavior, but the spatial correlations of these propensities do carry information about spatially heterogeneous dynamics. In short, the spatial structure of the propensity maps in Ref. [20] is important, but the color assigned to any specific particle is not.

B. Comparison with schematic model

We now generalize the simple model of Sec. III B to include spatial correlations. Following [4], we assume that particles diffuse independently, but with diffusion constants that are correlated over large spatial regions, each containing $n_c \gg 1$ particles. Since particles diffuse independently in any given run of the dynamics, it follows that $\langle f_i(t)f_j(t) \rangle_{\text{iso}} = \langle f_i(t) \rangle_{\text{iso}} \langle f_j(t) \rangle_{\text{iso}}$ for $j \neq i$, and hence:

$$\begin{aligned} \delta_{4,f}(t) &= n_c[F(2t) - F^2(t)] \\ \chi_{4,f}^{\text{iso}}(t) &= (1/2)[1 + F(4t) - 2F(2t)]. \end{aligned} \quad (10)$$

In this simple model, both $\delta_{4,f}(t)$ and $\chi_{4,f}(t)$ scale with n_c , while the isoconfigurational susceptibility $\chi_{4,f}^{\text{iso}}(t)$ is not sensitive to spatial correlations of the mobility and remains $\mathcal{O}(1)$. Thus, $\chi_{4,f}(t) \approx \delta_{4,f}(t) \gg \chi_{4,f}^{\text{iso}}(t)$, and hence $R_{4,f} \simeq 1$. This model shows that $R_{4,f}(t)$ becomes large if the lengthscale for dynamic heterogeneity is primarily structural in nature. The results of Fig. 2 therefore indicate that this is the case for the LJ system.

C. Comparison with a kinetically constrained model

We end with a brief discussion of the 1-FA model, which gives a useful theoretical insight into the quantities discussed above. As recalled in Sec. II, the model describes a dynamically heterogeneous material in which a few mobile excitations diffuse through an immobile background. Our simulations indicate that the ratios $R_P(t)$ and $R_{4,P}(t)$ have limiting forms at low T , which depend on dimensionality, d . In $1d$, the structure is very strongly correlated with the dynamics both locally and globally: $[R_P(\tau), R_{4,P}(\tau)] \approx [0.5, 0.7]$. However, in $3d$, the single

site ratio vanishes, $R_P(\tau) \approx 0$, while the global ratio is quite large, $R_{4,P}(\tau) \approx 0.4$. This occurs because the set of sites visited by a given excitation in $3d$ varies enormously from run-to-run. Using the initial positions of excitations to predict which sites will relax first in a given run is impossible. However, collective observables reveal that the rate of relaxation is reproducibly enhanced in regions with relatively many excitations (see also [25]).

This decoupling between the local and global ratios illustrates a situation in which the relation between dynamics and structure is only statistically significant at large length scales. Interestingly, this result is somewhat similar to that shown in Fig. 2 for the LJ system, although the microscopic mechanisms at work are presumably different. Moreover, preliminary studies indicate that the strong length scale dependence of predictability found in the 1-FA model is much less pronounced in models where kinetic constraints are stronger. In these other models, it appears that the dynamics on all length scales is strongly constrained by the initial structure.

V. OUTLOOK

We have investigated the degree to which structural fluctuations in glass-forming liquids influence their dynamical fluctuations. We defined $R_{4,f}$ and R_f which are quantitative measures of this influence, on long and short length scales respectively: they differ by nearly an order of magnitude in the LJ system at the lowest temperature considered. Thus, the influence of structure on dynamics is much stronger on long length scales than on short ones. This unexpected finding constitutes our main result.

Our work does not reveal which structural features are responsible for dynamic heterogeneity, but they do show that the search for such an observable should be undertaken at a coarse-grained level. This is consistent with recent studies [17, 18, 24, 25].

As a first step towards identifying a suitable coarse-grained structural quantity, we exploit the fact [7, 10, 22] that potential energy is correlated with dynamical heterogeneities (although correlations of the energy remain short-ranged). We compare fluctuations of the coarse-grained energy field, $\bar{\epsilon}_i(\ell)$, with those of the propensity. By coarse-graining on a length scale $\ell = 2$, so that $\ell \simeq \xi^{\text{prop}}$, we average away local fluctuations. We obtain a field that varies in space on a similar length scale to that of the dynamical propensity, and which reflects the average energy of different regions of the system. Interestingly, we find that regions with small energy are correlated with regions of low propensity for motion, as shown in Fig. 3e. While a more quantitative analysis is necessary before drawing firm conclusions, this correlation between energy and propensity is consistent with the strong local correlations between energy and dynamics demonstrated in [7, 10]. As an alternative to the energy, another promising route to a connection between structure and dynamics is provided by the presence of

extended modes characterizing the vibrational spectrum of amorphous materials [17, 18], and it would also be interesting to study connection between propensity and the locally ordered regions discussed in Ref. [35].

In any case, identifying the non-local structural features that are associated with mobile or immobile regions of glass-formers remains a central challenge.

Acknowledgments

We thank D. Chandler, J.P. Garrahan, P. Harrowell, L. Hedges, and D. Reichman for discussions. RLJ was

funded by NSF grant CHE-0543158 and LB by the Joint Theory Institute at the Argonne National Laboratory and the University of Chicago.

-
- [1] M.D. Ediger, C.A. Angell, and S.R. Nagel, *J. Phys. Chem.* **100**, 13200 (1996).
 - [2] M. D. Ediger, *Annu. Rev. Phys. Chem.* **51**, 99 (2000).
 - [3] W. Kob, C. Donati, S.J. Plimpton, P.H. Poole, and S.C. Glotzer, *Phys. Rev. Lett.* **79**, 2827 (1997).
 - [4] M.T. Cicerone, P.A. Wagner, and M.D. Ediger, *J. Phys. Chem. B* **101**, 8727 (1997).
 - [5] J. P. Garrahan and D. Chandler, *Phys. Rev. Lett.* **89**, 035704 (2002).
 - [6] S. Whitelam, L. Berthier and J.P. Garrahan, *Phys. Rev. Lett.* **92**, 185705 (2004).
 - [7] B. Doliwa and A. Heuer, *Phys. Rev. E* **67**, 031506 (2003); J. Qian, R. Hentschke, and A. Heuer, *J. Chem. Phys.* **111**, 10177 (1999).
 - [8] S. Franz, C. Donati, G. Parisi, and S.C. Glotzer, *Philos. Mag. B* **79**, 1827 (1999).
 - [9] C. Toninelli, M. Wyart, L. Berthier, G. Biroli, and J.-P. Bouchaud, *Phys. Rev. E* **71**, 041505 (2005).
 - [10] L. Berthier, G. Biroli, J.-P. Bouchaud, L. Cipelletti, D. El Masri, D. L'Hôte, F. Ladieu, and M. Pierno, *Science* **310**, 1797 (2005); L. Berthier, G. Biroli, J.-P. Bouchaud, W. Kob, K. Miyazaki, and D.R. Reichman, *J. Chem. Phys.* **126**, 184503 (2007); *ibid.*, **126**, 184504 (2007).
 - [11] P. Chaudhuri, L. Berthier, and W. Kob, *Phys. Rev. Lett.* **99**, 060604 (2007).
 - [12] G.H. Fredrickson and H.C. Andersen, *Phys. Rev. Lett.* **53**, 1244 (1984).
 - [13] G. Tarjus, S. Kivelson, Z. Nussinov, and P. Viot, *J. Phys.: Condens. Matter* **17**, R1143 (2005).
 - [14] G. Adam and J. H. Gibbs, *J. Chem. Phys.* **43**, 139 (1958).
 - [15] T.R. Kirkpatrick and D. Thirumalai, *Phys. Rev. Lett.* **58**, 2091 (1987); T.R. Kirkpatrick and P. Wolynes, *Phys. Rev. B* **36**, 8552 (1987); T.R. Kirkpatrick, D. Thirumalai and P. Wolynes, *Phys. Rev. A* **40**, 1045 (1987).
 - [16] W. Götze and L. Sjögren, *Rep. Prog. Phys.* **55**, 55 (1992);
 - [17] C. Brito and M. Wyart, *Europhys. Lett.* **76**, 149 (2006); C. Brito and M. Wyart, *J. Stat. Mech.* (2007) L08003.
 - [18] A. Widmer-Cooper, P. Harrowell, H. Perry and D.R. Reichman (unpublished).
 - [19] F. Stillinger and T. Weber, *Science* **225**, 983 (1984).
 - [20] A. Widmer-Cooper, P. Harrowell, and H. Fynewever, *Phys. Rev. Lett.* **93**, 135701 (2004); A. Widmer-Cooper and P. Harrowell, *J. Phys.: Cond. Matt.* **17**, S4025 (2005); *Phys. Rev. Lett.* **96**, 185701 (2006).
 - [21] A. Widmer-Cooper and P. Harrowell, *J. Chem. Phys.* **126**, 154503 (2007).
 - [22] G.S. Matharoo, M.S.H. Razul and P.H. Poole, *Phys. Rev. E* **74**, 050502 (2006).
 - [23] G.A. Appignanesi, J.A.R. Fris and M.A. Frechero, *Phys. Rev. Lett.* **96**, 237803 (2006); J.A. Rodriguez Fris, L.M. Alarcón, and G.A. Appignanesi, *Phys. Rev. E* **76**, 011502 (2007).
 - [24] D. Coslovich and G. Pastore, *Europhys. Lett.* **75**, 784 (2006).
 - [25] L.O. Hedges and J.P. Garrahan, *J. Phys.: Cond. Matt.* **19**, 205124 (2007).
 - [26] M.A. Frechero, L.M. Alarcón, E.P. Schulz, and G.A. Appignanesi, *Phys. Rev. E* **75**, 011502 (2007).
 - [27] M. T. Downton and M. P. Kennett, arXiv:0704.1497.
 - [28] W. Kob and H. C. Andersen, *Phys. Rev. Lett.* **73**, 1376 (1994).
 - [29] B.W.H. van Beest, G.J. Kramer, and R.A. van Santen, *Phys. Rev. Lett.* **64**, 1955 (1990).
 - [30] L. Berthier and W. Kob, *J. Phys.: Condens. Matter* **19**, 205130 (2007).
 - [31] L. Berthier, *Phys. Rev. E* **76**, 011507 (2007).
 - [32] Y. Jung, J. P. Garrahan and D. Chandler, *Phys. Rev. E* **69**, 061205 (2004).
 - [33] P. Harrowell, private communication.
 - [34] We obtain ξ^{prop} by collapsing S_4^{prop} onto a master curve, $S_4^{\text{prop}}(q, t)/S_4^{\text{prop}}(0, t) = f(q\xi^{\text{prop}})$, with $f(x) = 1/(1 + x^{\frac{2}{3}} + x^5)$ suggested by the numerical data [6, 9].
 - [35] D. Coslovich and G. Pastore, preprint arXiv:0705.0626 and arXiv:0705.0629.